



# COMPLEX SHAPE FORMING OF A FLAX WOVEN FABRIC; ANALYSIS OF THE TOW BUCKLING AND MISALIGNMENT DEFECT

Pierre Ouagne, D. Soulat, Julien Moothoo, Emilie Capelle, Sébastien Gueret

## ► To cite this version:

Pierre Ouagne, D. Soulat, Julien Moothoo, Emilie Capelle, Sébastien Gueret. COMPLEX SHAPE FORMING OF A FLAX WOVEN FABRIC; ANALYSIS OF THE TOW BUCKLING AND MISALIGNMENT DEFECT. Composites Part A: Applied Science and Manufacturing, 2013, 51, pp.1-10. hal-00838131

**HAL Id: hal-00838131**

**<https://hal.science/hal-00838131>**

Submitted on 24 Jun 2013

**HAL** is a multi-disciplinary open access archive for the deposit and dissemination of scientific research documents, whether they are published or not. The documents may come from teaching and research institutions in France or abroad, or from public or private research centers.

L'archive ouverte pluridisciplinaire **HAL**, est destinée au dépôt et à la diffusion de documents scientifiques de niveau recherche, publiés ou non, émanant des établissements d'enseignement et de recherche français ou étrangers, des laboratoires publics ou privés.

# COMPLEX SHAPE FORMING OF A FLAX WOVEN FABRIC; ANALYSIS OF THE TOW BUCKLING AND MISALIGNEMENT DEFECT

P. Ouagne<sup>1\*</sup>, D. Soulat<sup>2</sup>, J. Moothoo<sup>1</sup>, E. Capelle<sup>1,3</sup>, S. Gueret<sup>3</sup>

<sup>1</sup>Laboratoire PRISME University of Orleans, 8 rue Leonard de Vinci, 45072 Orleans, France

<sup>2</sup>GEMTEX, ENSAIT Roubaix 2 allée Louise et Victor Champier, 59056 Roubaix, France

<sup>3</sup>Groupe Depestele, BP 21, 14540 Bourguebus, France

\*Corresponding author: pierre.ouagne@univ-orleans.fr

## Abstract

With the view to minimise the impact on the environment and to produce structural parts with a good production-rate/cost-ratio, the sheet forming of woven flax based fabric was investigated in this study. A flax fibre plain-weave fabric has been used to form a complex tetrahedron shape. This shape is of particular interest as it contains several geometric singularities required by many automotive parts such as double or triple curvature and low-curvature edges. Globally, the complex tetrahedron shape was obtained, but tow buckling (out of plane bending of tows) was observed in specific zones of the shape. The main mechanism at the origin of this defect has been defined. A reduction of the tow buckle size was obtained by increasing the membrane tension. The influence of fabric architecture at the mesoscopic and macroscopic scales on the appearance of the tow buckles was demonstrated and discussed. Solutions to prevent the appearance of this defect based on the design of the fabric architecture at the tow or fabric scales were successfully proposed. As a consequence, when sheet forming of complex shapes is considered, specific fabric architectures should be chosen to prevent the appearance of the buckling defect.

**Keywords:** A. Textile forming; B. Natural fibres; C. Flax fabric; D. Buckling defect

## 1 Introduction

During the manufacturing of composite parts, defects may be introduced in their structure. Potter [1] has presented a taxonomy of defect states which may have adverse impacts on the performance of composite parts. This work concentrates specifically on the first step of the RTM process, the preforming stage of the dry reinforcements. In the Potter presentation [1], several defects can qualify this step as successful or unsuccessful drape. At the scale of the preform, denoted macroscale, it is possible to investigate if the preform shape is well obtained (if the preform fits to the tool in the case of sheet forming process), if wrinkles appear [2-6], if there is non-homogeneity of the fibre density in tows, or if a discontinuity of the preform due to sliding of tows takes place. It is also possible to study the mechanical state of the preform by quantifying the strain levels in different deformation modes (tension, in-plane shear). At the scale of the tows, meso-scale, other defects may appear. Tow misalignment in the plane of the fabric, [1] or out-of-plane misalignment also called tow buckles [4, 7] when some tows are not in contact anymore with the tool, can be investigated. All these defects have a strong influence on the resin flow impregnation because they modify the pore space and geometry within the fabric and therefore the in-plane and through-the-thickness permeability components [8-12]. They consequently impact the performance of the composite part [13, 14].

The draping behaviour of woven fabrics in the textile industry [15, 16] is usually characterized by a drapmeter [17, 18]. It is only associated with the bending behaviour of the fabric. However, in the case of shapes with double or triple curvatures, coupled deformation in the woven structures during the process takes place and cannot be analysed by the single bending indicator. This is even more the case if specific architectures such as non-crimped fabrics NCF [3, 19] or 3D-Interlock for examples [20, 21] are used. Consequently several numerical approaches, using the finite element method, have been extensively used to investigate the draping behaviour of fabric on specific tools

[22-29]. These mechanical approaches, based on the finite element method, take into account the complex mechanical behaviour of dry fabrics. They are designed to analyse the effect of the process parameters on the feasibility to preform woven fabrics without defects. In the case of the sheet forming process, sliding conditions within the tool and the pressure of the blank-holders are generally considered. In these approaches several criteria are used to detect, control or prevent the wrinkling phenomenon. The most widely used is the detection by the locking shear angle [25, 30]. Other approaches can also be considered. One of them is based on the deactivation of elements in compression [31]. Another one is based on the wrinkling energy [32, 33] and takes into account shear, tension and bending deformations. If wrinkles, at the macroscale, can be detected by these criteria, defects at the micro and meso scales are more difficult to study and quantify, especially on complex shapes (with double-curved shapes and triple-point curvature for example). Recent experimental works [6, 34-36] have shown the apparition of some tow buckles in the preform. This defect is also called tow distortion by Potter et al [1]. These tow buckles are the consequence of a specific in-plane bending behaviour of tows subjected to biaxial-tension deformations during the preforming process. Few studies have investigated the effect of the architecture of the woven fabrics on the tow buckling. It is therefore proposed in this paper to investigate, using an experimental approach, the influence of the woven flax fabric architecture on the preforming quality of a complex shape. Natural fibres have long been considered as potential reinforcing materials or fillers in thermoplastic or thermoset composites. Numerous studies deal with the subject [37-42]. Natural fibres are particularly interesting because they are renewable, have low density and exhibit high specific mechanical properties. They also show non-abrasiveness during processing, and more importantly biodegradability. Studies at the composite scale also enable focussing on the life-cycle assessment of the part and on the complete energetic record linked to the use of the natural fibres. Dissanayake *et al.* [43,44] analysed the energy used in the production of flax fibres for the reinforcement of composites. They showed, in the case of traditional production of flax mats, with the use of synthetic fertilizers and pesticides associated with traditional fibre extraction such as dew

retting and hackling, that the energy consumption linked to the production of a flax mat is comparable to the energy consumed during the production of a glass mat. They also concluded that the spinning of fibres for the production of yarns typically used for the production of woven fabrics is an energy intensive operation. In that case, the glass woven fabric may appear superior to a flax woven fabric if one considers an environmental energy viewpoint. They also recommended designing new architectures of woven fabrics from aligned fibres tows, as it is the case for the reinforcement studied in this work, instead of spun yarns. A large amount of work has been devoted to identify the tensile behaviour of individual fibres or a group of a few fibres of different nature and origin [45-48]. However, few studies deal with the subject of the mechanical behaviour of fibre assemblies and particularly analyse the deformability of these structures.

This paper therefore proposes to analyse the feasibility of forming the mentioned complex shape with flax-fibre woven-fabric reinforcements. A special attention is given on the defects that may appear during forming. The tow buckling defect is particularly discussed and solutions on ways to prevent their appearance in relation to the fabric architecture at the macro and meso scale are presented.

## 2 Experimental procedures

### 2.1 Tested materials

Generally, when natural fibres are considered, twisted yarns are used to increase the tensile properties. Indeed, as discussed by Goutianos *et al.* [49] sufficient tensile properties of the yarns are necessary for these materials to be considered for textile manufacturing or for processes such as pultrusion or filament winding. However, spinning, as mentioned previously consumes large amounts of energy [43] and this cannot be beneficial for natural fibre based reinforcement. Moreover, Goutianos *et al.* [50] also showed that the mechanical properties of composites manufactured from spun yarns exhibit lower mechanical properties than the ones manufactured from flat tows. As a consequence, three reinforcements made from untwisted tows with different architectures at the macro and microscopic scales were selected for the current research.

The first flax fabric (Figure 1) used in this study, is a plain-weave fabric with an areal weight of  $280 \pm 19 \text{ g/m}^2$ , manufactured by Groupe Depestele (France) from untwisted tows. In this fabric, the fibres or groups of fibres are slightly entangled to provide a minimum rigidity to the tows. This geometry has been chosen as it generates low bending stiffness tows, therefore limiting the crimp effect in the fabric, and therefore, limiting empty zones between tows. It has also been chosen because the tow permeability is higher than the highly twisted yarn permeability making them more suitable for the LCM (Liquid Composite Moulding) process. The fabric is not balanced, as the space between the weft tows ( $1.59 \pm 0.09 \text{ mm}$ ) is different from the one between the warp tows ( $0.26 \pm 0.03 \text{ mm}$ ). The width of the warp and the weft tows are respectively  $2.53 \pm 0.12 \text{ mm}$  and  $3.25 \pm 0.04 \text{ mm}$ . As a consequence, there are 360 warp tows and 206 weft tows per metre of fabric. The lineal masses of the warp and the weft tows are the same and are equal to  $494 \pm 17 \text{ g/km}$ . The tows are constituted by globally aligned groups of fibres. The length of these groups of fibres varies between 40 to 600 mm with a maximum occurrence at 80 mm. This reinforcement was originally developed to manufacture large panels with low curvature and was therefore not designed for complex shape forming.

A second reinforcement was tested in this work. It is a plain-weave fabric with an areal weight of  $458 \pm 9 \text{ g/m}^2$ , also manufactured by Groupe Depestele (France). The fabric is also made of rectangular flat tows (Figure 2). No space is visible between the weft tows whereas the space between the warp tows is  $0.43 \pm 0.09 \text{ mm}$ . The width of the warp and the weft tows are respectively  $2.0 \pm 0.2 \text{ mm}$  and  $2.7 \pm 0.3 \text{ mm}$ . As a consequence, there are 403 warp tows and 370 weft tows per metre of fabric. The linear mass of the warp and the weft tows are respectively for the warp and weft tows:  $551 \pm 8$  and  $624 \pm 10 \text{ g/km}$ .

The third reinforcement (Figure 3) is a hopsack with an areal weight of  $508 \pm 11 \text{ g/m}^2$  manufactured by Composites Evolution Company [51]. This fabric is comprised of tows woven according to a plain-weave style. The tows are themselves constituted of four parallel untwisted yarns placed close together as shown in Figure 3. The round yarns are manufactured from aligned fibres held together by a polyester yarn going in a spiral manner along the flax yarn. The space between the weft tows ( $1.53 \pm 0.08 \text{ mm}$ ) is different from the one between the warp tows ( $0.59 \pm 0.04 \text{ mm}$ ). The width of the warp and the weft tows are respectively  $3.14 \pm 0.08 \text{ mm}$  and  $3.08 \pm 0.08 \text{ mm}$ . As a consequence, there are 268 warp tows and 216 weft tows per metre of fabric.

## 2.2 Experimental setup

A device specifically designed to analyse the local strains during the forming of reinforcement fabrics [34, 52] is presented in Figure 4.a. The mechanical part consists of a punch/open die couple and a classical blank-holder system. The punch used in this study (Figure 4.b) is a tetrahedron form with 265 mm sides. Its total height is 128 mm and the base height is 20 mm. The edges and vertices possess 10 mm radius for the punch and 20 mm for the die. Due to the low value of the edges radius, the expected shapes should be highly double curved and large strains are expected to take place along the edges. The die used with this punch is a triangular open die ( $314 \times 314 \times 314 \text{ mm}^3$ ).

The die is open to allow for the measurement of the local strains during the process with video cameras associated to a marks tracking technique [53]. The motion of the punch is given by a piloted electric jack. The punch velocity is 30 mm/min and its stroke 160 mm. The maximum depth of the punch is 160 mm. To avoid wrinkling defects during the preforming tests, it is possible to introduce tension on the fabric by a classical multi-part blank-holder. It is composed of independent blank-holders actuated by pneumatic jacks that are able to impose and sense independently a variable pressure. Dimensions, positions, and specifically variable pressure on each of these blank-holders can be easily changed to investigate their influence on the quality of the final preform [32, 52]. An initial square specimen of the flax fabric is positioned between the die and the six blank-holders placed on specific locations around the tetrahedron punch. The initial positioning of the fabric is of importance. This partly conditions the final yarns orientation within the part and as a consequence its mechanical stiffness. Due to the tetrahedral geometry of the punch, it is not possible to place the fabric in order to foresee a specific orientation of the tows in the final shape. For the tests presented in this paper, it was chosen to align the warp or the weft tows with an edge of the tetrahedron (Figure 5). Before applying the blank holder pressure, and before starting the movement of the punch, the fabric can bend under its own weight. It is therefore necessary to apply some tensions at the tow extremities using a drawbead system. At the end of the preforming test, global analysis (dimensions, defects etc.) can be performed on the final state of the preform before removing it from the tool. The preform can be fixed by applying a spray of resin on its surface so that the preform can be removed from the tools and kept in its final state.

Using this device, an experimental study to analyse with this precise shape, the generation of defects and specifically the buckles of tows and their location (on faces, edges and around the triple point) is carried out. The influence of process parameters such as the initial orientation of the fabric (Figure 5), the applied blank-holder pressure (between 1 and 5 bar) are also considered and



analysed. The justification of the applied blank-holder pressures are indicated in the Result part of this document.

### **3 Results**

#### *3.1 Description of defects*

The first tests were conducted on reinforcement 1. The initial position of the reinforcement is  $0^\circ$  (Figure 5a) and a uniform 1 bar pressure was applied to the fabric by each blank-holder to avoid exposing the tows to large tensile strains [35]. The global preform shape was obtained without the presence of defects such as wrinkles or discontinuities (sliding of tows in the useful zone). Out of the useful zone, some wrinkles can be observed (Figure 6.a) around the preform and around the blank-holders.

More locally, on faces and edges, two types of defects can be noticed. The first one is characterised by some material over-thickness zones which are the consequence of buckles generated by some tows perpendicular to the one passing by the top of the tetrahedron shape. These buckle zones converge to the triple point (top of the tetrahedron) from the bottom of the shape depending on the initial orientation of the fabric. This buckling phenomenon cannot be acceptable in terms of preform quality for composite part manufacturing as the homogeneity of the thickness preform is not controlled. For this first test, buckles or tow buckling (Figures 6.b, 6c) appear on the middle of the face 3 and on one edge (denoted edge 1 between faces 1 and 2) of the formed tetrahedron shape (Figure 7). No buckles are observed on faces 1 and 2.

The second type of defect, localised on faces of the tetrahedron, concerns the alignment of tows. The trajectories of tows perpendicular to the one passing by the top of shape show a specific curvature due to a bending deformation state. This misalignment could be considered as a defect because this final tow orientation is not controlled on these faces. This misalignment appears on the three faces of the tetrahedron shape.

An experimental approach was also used to investigate a possible link between the two defects (tow buckles and tow misalignment). For example, the specific curvature of the bent tows could be considered as a criterion to predict the appearance of the buckling defect. Measurements of these two types of defects are conducted on preforms, shaped using the experimental device with controlled parameters. For the buckles it consists of measuring the height of the over-thickness. These measurements are conducted manually on preforms. The bending angles associated with the curvature of the tows (Figure 6b) were measured on the same tows from pictures of the faces taken on three different shapes. Image analysis using the software GIMP was used to perform the measurements that were validated by local manual measurements. All the reported data are the mean values of the measured parameters.

### *3.2 Influence of process parameter on the defects for reinforcement 1*

To investigate the influence of the process parameters on the generation of defects during the sheet forming process, other tests on the first reinforcement were conducted. The variations of the initial fabric orientation as well as the blank holder pressure are considered.

For the test conducted with the orientation  $90^\circ$  (Figure 5b) and for a uniform blank-holder pressure of 1 bar, buckles appear on faces 1 and 2 (Figure 8), and not on face 3 and edge 1 as was the case for orientation  $0^\circ$ . Curvature of tows, as was the case for orientation  $0^\circ$ , can be observed on the three faces. Values of bending angle for these two tests under the same blank-holder pressure are reported in Figure 9, with a precision of  $\pm 4^\circ$ . If one considers the measurement errors, the measured bending angles are situated in the same range of values for the three faces. No real tendency can be extracted from these measurements as the bending angles are similar in faces where the buckles occur and in the faces where buckles do not appear. The magnitude of the bending angle within our testing conditions (1 bar blank-holder pressure) is therefore not responsible for the changes of the buckle zone location for the two tested orientations whereas the

initial reinforcement orientation seems to be crucial. As a consequence, bending of the tow in its plane does not appear to be a sufficient criterion to predict the appearance of the buckles.

At the fabric scale, the appearance of these defects is probably due to a combination of parameters: in-plane bending of the tows perpendicular to those passing by the triple point, the architecture of the woven fabric, but also the process parameter which may also play a role in the occurrence of these defects. Indeed for the tetrahedron shape, the tows passing by the triple point are tighter than the perpendicular ones, and an investigation upon the effect of the increasing tension by the evolution of the blank-holder pressure on the occurrence of the buckles has been carried out. For the  $0^\circ$  orientation, the evolution of the bending angles on the three faces of the tetrahedron shape as a function of the increasing blank-holder pressure is reported in Figure 10. It shows that the bending angle measured on face 3 decreases as a function of the increasing blank-holder pressure. This decrease in the bending angle is probably due to the increasing tensile deformation of the tows passing by the triple point [35, 36]. In this case, the perpendicular tows are dragged by the tows passing by the triple point in the direction of the top of the preform. The lower variations observed on faces 1 and 2 are probably more due to measurement dispersion and to their relative inaccuracy. As a consequence, it can be concluded that the control of the tows orientation by only varying the blank-holder pressure is not possible on this complex shape.

Associated with the tow orientation tests, the heights of the buckles, measured on edge 1 and face 3 for the  $0^\circ$  orientation and on faces 1 and 2 for the  $90^\circ$  orientation, are reported as a function of the increasing uniform blank-holder pressure in Figure 11. The precision of these measurements is about  $\pm 0,1$  mm. A reduction of the buckle size on the edge 1 as a function of the increasing global blank-holder pressure is observed. This reduction is due to the higher tension of the tows exhibiting buckles. In the other zones, the influence of the blank-holder on this defect is not significant.

Differential blank-holder pressures were also applied for the  $0^\circ$  orientation to locally increase the tension on the tows exhibiting the buckles. In a first series of tests, the pressure of blank-holders 1

and 6 (large ones Figure 7.b) was increased, and the pressures of the other blank-holders remained at 1 bar. In a second series of tests, the pressure of blank-holders 2, 4 and 5 (small ones) was raised and the other pressures were maintained to 1 bar. Figure 12 summarises the results obtained for the height of buckles on face 3 and edge 1 for the first test (denoted by BH-1-6) and the second test (denoted by BH-2-4-5). When the pressure of blank-holders 1 and 6 was raised, and the pressures of the others were maintained at 1 bar, the sizes of the buckles decreased on edge 1 and remained constant on Face 3. Once again, one may suppose that the decrease of the buckle size on edge 1 is due to the rise of the tension in the tows forming the buckles. When the pressure of blank-holders 2, 4 and 5 (small ones) was increased and the pressure of the large ones was maintained to 1 bar, the size of the buckles remained constant on edge 1 but decreased on Face 3. The decrease in Face 3 is probably due to the fact that the tension is raised in the tows perpendicular to the ones passing by the triple point forming the buckles. It can be concluded that the tension of these tows is widely controlled by the small blank-holders whereas the blank-holders 1 and 6 control the tension of the tows perpendicular to the edge 1.

The results presented in the previous paragraphs with the goal to reduce the occurrence or the size of the buckles show that the rise of the small blank-holder pressure, corresponding to a reduction of the fabric movement in the corner and to an increase of the tension in the tows passing by these blank-holders, slightly reduces the buckle size on Face 3. In this case, the size of the buckle does not change on edge 1. If one increases the pressure of blank-holders 1 and 6, the size of the buckles decreases on edge 1, whereas it is not affected on Face 3. It seems therefore difficult to simultaneously decrease the buckles size on Face 3 and on edge 1. It is also interesting to note that a global blank-holder pressure increase has the same effect on the buckle size on edge 1 and face 3 as an increase of pressures of blank-holders 1 and 6 only. As a consequence of the previous observations, it seems to be difficult to decrease the size of the buckles on face 3 and on edge 1, and

by extension to stop the occurrence of the buckling phenomenon, by only working with the blank-holder pressure using reinforcement 1 for both orientations  $0^\circ$  and  $90^\circ$  in our test configuration.

It has to be noticed that the blank-holder pressure was not raised above values of 2.5 bar as another defect (sliding of tows within the membrane) appears in this case as illustrated by Figure 13.

### *3.3 Global preform analysis: Reinforcement 2*

When reinforcement 2 is used, the global shape is also obtained (Figure 14). No apparent defect such as wrinkles and sliding of tows within the structure can be observed. Small buckles may appear on edge 1 if very low blank-holder pressure is applied (Figure 14). However, this phenomenon can be prevented by applying enough blank-holder pressure. In our case, a global blank-holder pressure of 1.5 bar was sufficient. Tow misalignment can also be observed on the three faces of the shape. The bending angles are situated in a similar range of values as for reinforcement 1 ( $142^\circ \pm 2$ ,  $142^\circ \pm 1$ ,  $138^\circ \pm 2$  for faces 1, 2, 3 respectively). It is also interesting to notice that the sliding of a tow within the woven structure did not appear up to a global blank-holder pressure of 5 bar.

The experimental conditions used to test reinforcement 2 were similar to the ones used for reinforcement 1. As a consequence, the structure of the reinforcement at the scale of the tows and at the scale of the fabric (architecture of the fabric) is responsible for the different behaviours and particularly by the fact that no buckles appear on faces or on edges if enough blank-holder pressure is applied.

### *3.4 Global preform analysis: Reinforcement 3*

Figure 15 shows that the global tetrahedron shape is achieved using reinforcement 3. As for reinforcement 2, no apparent defect such as wrinkles and sliding of tows takes place (Figure 15). Very small buckles can be observed on edge 1 at low blank-holder pressure, but this defect can be prevented by applying a global blank-holder pressure higher than 2 bar. Tow misalignment also

takes place in the three faces. The values of the bending angles are situated in the same range of values as for reinforcements 1 and 2 ( $141^{\circ} \pm 1$ ,  $142^{\circ} \pm 2$ ,  $146^{\circ} \pm 1$  for faces 1, 2, 3, respectively).

#### **4 Discussion: solutions to prevent the appearance of buckles**

The main mechanism controlling the appearance of the buckling phenomenon is the bending of flat tows in their own plane. This mechanism is difficult to accommodate. So buckling of the tow takes place. The tows exhibiting buckles are not tight. Increasing the global blank-holder pressure to tighten the whole membrane or increasing selected blank-holder pressures to tighten the tow exhibiting buckles showed that the size of the buckles decreased in localized zones but not in the whole buckled areas. Moreover, the buckles did not disappear even though their size was locally reduced. This therefore means that it has not been possible to prevent the appearance of buckles using reinforcement 1 by just varying the process conditions with our set of blank-holders.

The localisation of the buckles was shown to be different depending on the initial orientation of the fabric on the preforming device. This dependence on initial orientation suggests that the occurrence of the buckles depends on the macroscopic architecture of the fabric. Reinforcement 1, considered in this study, is an unbalanced plain-weave fabric. The tows, used in the warp and the weft directions are similar, but a space between the weft tows (about the width of a tow) is observed on the fabric, whereas this space is not present between the warp tows. As buckles only appear when the warp tows bend in their plane in zones where the weft tows are vertical, (face 3 and edge 1 orientation  $0^{\circ}$  and face 1 and face 2 orientation  $90^{\circ}$ ) one can conclude that the architecture of the reinforcement is a key parameter for conditioning the appearance of the buckles. When the warp tows are vertical (without any space between them) the buckles do not appear even though the horizontal tows exhibit the same amount of bending. This phenomenon suggests that the presence of the space between the weft tows is one of the parameters that control the appearance of the buckles. Indeed, if the vertical tows are placed close together without any space between them, the

buckles do not have any space to appear. As a consequence, one can expect that a balanced woven fabric with no space between the warp and the weft tows should not show the appearance of buckles. This hypothesis was tested with success on reinforcement 2, which was specially manufactured by Groupe Depestele to prevent the appearance of the buckles. This reinforcement is a balanced plain-weave fabric also manufactured from flat untwisted tows. This result suggests that it is possible to preform the tetrahedron shape without any buckling defect if an optimised architecture, without any space between the warp and the weft tows, is considered.

The occurrence of buckles therefore depends on the shape to be formed because the shape may induce bending of the tows not only in their own plane but also on the architecture at the macroscopic scale of the fabric. At the mesoscopic scale, the architecture of the tows is also a parameter to take into account. Indeed the tows of reinforcement 3 submitted to similar bending angles than the tows of reinforcement 1 do not exhibit buckles even though the fabric is unbalanced with some spaces observed between the tows. The hypothesis of tows placed closed together like for reinforcement 2 cannot be considered. However, the tows of reinforcement 3 are not constituted by aligned tows. The rectangular tow is comprised of four “cylindrical” yarns aligned close together. Due to the composition of the tows, themselves made of cylindrical yarns, the bending deformation of the tow in its plane can be accommodated without the formation of buckles. This therefore means that it is possible to preform a complex shape such as the tetrahedron by using an appropriate design of the architecture of the fabric at the mesoscopic scale (scale of the tow).

If it has been possible to prevent the occurrence of buckles by adapting the architecture of the reinforcement either at the macroscopic scale (reinforcement 2) or at the mesoscopic scale (reinforcement 3), it is important to bear in mind that the energy required to produce the reinforcement should be kept to a minimum, at least lower to the energy necessary to produce equivalent glass reinforcements to minimise the impact on the environment. Woven fabrics with

aligned fibre tows such as reinforcement 1 and 2 are recommended [43, 44]. The case of reinforcement 3 is more questionable as an extra yarn production step is necessary to produce it. However, it is difficult to conclude on that issue without performing a global life-cycle assessment on the 3 reinforcements.

For the considered tetrahedron shape, tow misalignment takes place on the three faces of the three considered woven reinforcements. The in-plane bending observed in faces is the consequence of the complex punch geometry, and it is interesting to notice that the in-plane bending angles are situated in the same range of values for the three reinforcements despite the fact that their architectures are different at the macro and mesoscopic scales.

This study was of a preliminary nature on the subject, as the blank-holder pressures and geometries were not optimised. It would therefore be very interesting to investigate the effect of the blank-holders shape and pressures with specifically designed tools on the appearance of the buckling defect. A whole series of complex shapes should also be performed to investigate the presence of defects such as buckles and misalignment and the mechanisms associated to their appearance.

## **5 Conclusions**

To increase the possible development of the natural fibre composites to complex shape parts, this study investigated the possibility to preform, using the sheet-forming process, a highly complex shape with a triple curvature without defect from the selected reinforcements. An unbalanced plain-weave fabric (reinforcement 1) was first studied. The global tetrahedron shape was obtained, but this study showed that defects such as buckles are present and that it is not possible to predict the final tow orientation due to misalignments. This experimental study showed that the control of these defects by non optimised blank-holder pressure is difficult due to the complexity of the coupled



strains taking place during the preforming step, especially on a highly complex shape. By testing several architectures of fabric, experimental observations demonstrated that it was possible to prevent the occurrence of buckles by designing or selecting specific reinforcement architectures. Another plain-weave fabric, (reinforcement 2) was designed for this goal. The warp tows, as well as the weft tows are respectively aligned close together (without any space between two consecutive tows). By specifically working on the reinforcement architecture at the macroscopic scale, the expected shape was obtained without any defect.

It has also been demonstrated that it was possible to obtain the tetrahedron shape without any buckling defect with an unbalanced hopsack made from highly deformable tows that can accommodate bending in their own plane.

It is, however, important to notice that a reinforcement designed for a specific application may not be applicable for forming another shape. Consequently this experimental study has shown the influence of the choice of the reinforcement architecture on the deformation limits during the preforming step. The manufacturers need to offer large ranges of reinforcements, designed to accommodate the specific deformation modes and amplitudes imposed by the shape to form.

## Références

- [1] Potter K, Khan B, Wisnom M, Bell T, Stevens J. "Variability, fibre waviness and misalignment in the determination of the properties of composite materials and structures" *Composites: Part A* 2008; 39: 1343–1354.
- [2] Bloom LD, Wang J, Potter KD. Damage progression and defect sensitivity: An experimental study of representative wrinkles in tension. *Composites: Part B* 2013; 45: 449-458.
- [3] Lee J, Hong S, Yu W, Kang T. The effect of blank holder force on the stamp forming behavior of non-crimp fabric with a chain stitch. *Compos. Sci. Technol* 2007; 67:357-366.
- [4] Lin H, Wang L, Long AC, Clifford MJ, Harrison P. Predictive modelling for optimization of textile composite forming. *Compos Sci Technol* 2007; 67: 3242–3252.
- [5] Sharma SB, Sutcliffe MPF, Chang SH. "Characterisation of material properties for draping of dry woven composite material" *Composites: Part A*, 2003; 34: 1167-1175.
- [6] Ouagne P, Soulat D., Hivet G, Allaoui S, Duriatti D. Analysis of defects during the performing of a woven flax. *Advanced Composites Letters* 2011; 20: 105-108.
- [7] Prodromou AG, Chen J. (1997) On the relationship between shear angle and wrinkling of textile composite preforms. *Composites: Part A* 1997; 28: 491– 503.
- [8] Walther J, Simacek P, Advani SG. The effect of fabric and fiber tow shear on dual scale flow and fiber bundle saturation during liquid molding of textile composites. *Intern J of Mater Form*, 2012; 5: 83-97.
- [9] Arbter, R., Beraud, J.M., Binetruy, C, Bizet, L, Bréard, J, Comas- Cardona, S, Demaria, C, Endruweit, A, Ermanni, P, Gommer, F, Hasanovic, S, Henrat, P, Klunker, F, Laine, B, Lavanchy, S, Lomov, SV, Long, A, Michaud, V, Morren, G, Ruiz, E, Sol, H, Trochu, F, Verleye, B, Wietgreffe, M, Wu, W, Ziegmann, G. Experimental Determination of the Permeability of Textiles: A Benchmark Exercise. *Composites Part A*, 2011; 42: 1157-1168.
- [10] Hou Y, Comas-Cardona S, Binetruy C, Drapier S. Gas transport in fibrous media: Application to in-plane permeability measurement using transient flow. *J Compos Mater* 2012, doi: 10.1177/0021998312455676.
- [11] Ouagne P, Bréard J. Continuous transverse permeability of fibrous media. *Composites: Part A* 2010; 41: 22-28.
- [12] Ouagne P, Ouahbi T, Park C-H, Bréard J, Saouab A. Continuous measurement of fiber reinforcement permeability in the thickness direction : Experimental technique and validation. *Composites: Part B* 2012; 45: 609-618.
- [13] Lee SH, Han JH, Kim SY, Youn JR, Song YS. Compression and Relaxation Behavior of Dry Fiber Preforms for Resin Transfer Molding. *J. Compos. Mater.* 2010; 44: 1801-1820.
- [14] Skordos AA, Aceves CM, Sutcliffe MPF. A simplified rate dependent model of forming and wrinkling of pre-impregnated woven composites. *Composites: Part A* 2007; 38: 1318–1330.
- [15] Abdin, Y, Taha, I, El-Sabbagh, A, Ebeid, S, Description of Draping Behaviour of Woven Fabrics Over Single Curvatures by Image Processing and Simulation Techniques, *Composites: Part B* 2013; 45: 792-799.
- [16]. Sule G. Investigation of bending and drape properties of woven fabrics and the effects of fabric constructional parameters and warp tension on these properties. *Textile Research Journal* 2012; 82: 810–819.
- [17] Peirce FT. The "handle" of cloth as a measurable quantity. *Journal of the Textile Institute Transactions* 1930; 21: 377-416.
- [18] Cusick GE. The measurement of fabric drape. *J Text. Inst.* 1968; 59(6): 253–260.
- [19] Bel S, Hamila N, Boisse P, Dumont F. Finite element model for NCF composite reinforcement preforming: Importance of inter-ply sliding, *Composites: Part A* 2012; 43: 2269-2277.
- [20] De Luycker E, Morestin F, Boisse P, Marsal D. Simulation of 3D interlock composite preforming. *Compos. Struct.* 2009; 88: 615-623.
- [21] De Luycker E, Morestin F, Boisse P, Marsal D Numerical Analysis of 3D Interlock Composite Preforming. I *Intern J of Mater Form* 2008; 1: 843-846.

- [22] Hamila N, Boisse P. Simulations of textile composite reinforcement draping using a new semi-discrete three node finite element. *Composites: Part B* 2008; 39: 999–1010.
- [23] Gereke T, Döbrich O, Hübner M, Cherif C. Experimental and Computational Composite Textile Reinforcement Forming: A Review, *Composites: Part A* 2013; 46: 1-10.
- [24] Khan MA, Mabrouki T, Vidal-Sallé E, Boisse P. Numerical and experimental analyses of woven composite reinforcement forming using a hypoelastic behaviour. Application to the double dome benchmark. *J Mater Process Technol* 2010; 210: 378- 388.
- [25] Peng X, Rehman ZU. Textile composite double dome stamping simulation using a non-orthogonal constitutive model. *Compos Sci Technol* 2011; 71: 1075-1081.
- [26] Yu WR, Pourboghrat F, Chung K, Zampaloni M, Kang TJ. Non-orthogonal constitutive equation for woven fabric reinforced thermoplastic composites. *Composites: Part A* 2002; 33: 1095-1105.
- [27] Peng XQ, Cao J. A continuum mechanics-based non-orthogonal constitutive model for woven composite fabrics. *Composites: Part A* 2005; 36: 859-874.
- [28] Peng X, Ding F. Validation of a non-orthogonal constitutive model for woven composite fabrics via hemispherical stamping simulation. *Composites A* 2011; 42: 400-407.
- [29] Charmetant A, Vidal-Sallé E, Boisse P. Hyperelastic modelling for mesoscopic analyses of composite reinforcements. *Compos Sci Technol* 2011; 71: 1623-1631.
- [30] Boisse P, Hamila N, Vidal-Sallé E, Dumont F. Simulation of wrinkling during textile composite reinforcement forming. Influence of tensile, in-plane shear and bending stiffnesses. *Compos. Sci. Tech.* 2011; 71: 683-692.
- [31] Skordos AA, Sutcliffe MPF. Stochastic simulation of woven composites forming. *Compos Sci Tech* 2008; 68: 283–296.
- [32] Zhu B, Yu TX, Zhang H, Tao XM. Experimental investigation of formability of commingled woven composite preform in stamping operation. *Composites: Part B* 2011; 42 :289-295.
- [33] Zhu B, Yu TX, Teng J, Tao XM. Theoretical Modeling of Large Shear Deformation and Wrinkling of Plain Woven Composite. *J Compos Mater* 2009; 43: 125-138.
- [34] Allaoui S, Boisse P, Chatel S, Hamila N, Hivet G, Soulat D, Vidal- Salle E. Experimental and numerical analyses of textile reinforcement forming of a tetrahedral shape. *Composite Part A* 2011; 42: 612- 622.
- [35] Ouagne P, Soulat D, Tephany C, Duriatti D, Allaoui S, Hivet G. Mechanical characterisation of flax based woven fabrics and in situ measurements of tow tensile strain during the shape forming. *J Compos Mater*, doi:10.1177/0021998312467217.
- [36] Capelle E, Ouagne P, Tephany C, Soulat D, Duriatti D, Gueret S. Analysis of the tow buckling defect during the complex shape forming of a flax woven fabrics. – Proceedings of the 15TH EUROPEAN CONFERENCE ON COMPOSITE MATERIALS, Venice, Italy, 24-28 June 2012.
- [37] La Mantia FP, Morreale M. Green composites: A brief review. *Composites: Part A* 2011; 42: 579-588.
- [38] Satyanarayana KG, Arizaga G, Wypych F. Biodegradable composites based on lignocellulosic fibers—An overview *Prog in Polym Sci* 2009; 34: 982–1021.
- [39] Biagiotti J, Puglia D, Kenny JM. A Review on Natural Fibre-Based Composites-Part I. *J of Nat Fib* 2004; 1: 37-68.
- [40] Puglia D, Biagiotti J, Kenny JM. A Review on Natural Fibre-Based Composites—Part II, *Journal of Natural Fibers* 2005; 2: 23-65.
- [41] Pandey JK, Ahn SH, Lee CS. Mohanty AK. Misra M. Recent Advances in the Application of Natural Fiber Based Composites *Macromol Mat and Eng.* 2010; 295: 975–989.
- [42] Ouagne P, Bizet L, Baley C, Bréard J. Analysis of the Film-stacking Processing Parameters for PLLA/Flax Fiber Biocomposites. *J Compos Mater* 2010; 44: 1201-1215.
- [43] Dissanayake N, Summerscales J, Grove S, Singh M. Life Cycle Impact Assessment of Flax Fibre for the Reinforcement of Composites. *J Biobased Mat and Bioener* 2009; 3: 245-248.
- [44] Dissanayake, N.; Summerscales, J.; Grove, S.; Singh, M. Energy use in the production flax fiber for the reinforcement of composites *J Natur Fib* 2009; 6: 331-346.

- [45] Baley C. Analysis of the flax fibres tensile behaviour and analysis of the tensile increase” Composites: Part A 2002; 33: 2143-2145.
- [46] Bodros E, Baley C. Study of the tensile properties of stinging nettle fibres. Materials Letter 2008; 62: 2143-2145.
- [47] Alawar A, Hamed AM, Al-Kaabi K. Characterization of treated date palm tree fiber as composite reinforcement. Composites: Part B 2009; 40: 601-606.
- [48] Kim JT, Netravili AN. Mercerization of sisal fibers: Effects of tension on mechanical properties of sisal fibers and fiber-reinforced composites. Composites: Part A 2010; 41: 1245-1252.
- [49] Goutianos S, Peijs T. The optimization of flax fibre yarns for the development of high-performance natural fibre composites. Advanced Composite Letters 2003; 12: 237-241.
- [50] Goutianos S, Peijs T, Nystrom B, Skrifvars M. Development of flax based textile reinforcements for composite applications. A Compos Mat 2006; 13: 199–215.
- [51] [www.compositesevolution.com](http://www.compositesevolution.com)
- [52] Soulat D, Allaoui S, Chatel S. Experimental device for the optimization step of the RTM process. Int J Mat Form 2009; 2: 181–184.
- [53] Bretagne N., Valle V., Dupré JC. “Development of the marks tracking technique for strain field and volume variation measurements“. *NDT&E International*, 38 (2005) 290-298.

## Figure Captions

- Figure 1: Architecture of reinforcement 1 at the scales of the fabric and the tow.
- Figure 2: Architecture of reinforcement 2 at the scales of the fabric and the tow.
- Figure 3: Architecture of reinforcement 3 at the scales of the fabric, the tow and the yarn.
- Figure 4: a) The sheet forming device and b) the tetrahedron punch
- Figure 5: Initial positioning of the woven fabric
- Figure 6: Forming of reinforcement 1: a) Wrinkles outside of the useful zone; (b) Position of the buckles and bending angle measurement; (c) Focus on the buckles
- Figure 7: Localisation of the buckle zone for initial fabric orientation of  $0^\circ$
- Figure 8: Localisation of the buckle zone for initial fabric orientation of  $90^\circ$
- Figure 9: Influence of the initial fabric orientation on the tows curvature for reinforcement 1
- Figure 10: Influence of the global blank-holder pressure on the tows curvature for reinforcement 1
- Figure 11: Influence of the initial fabric orientation and the global Blank-holder pressure on the size of the buckles for reinforcement 1
- Figure 12: Influence of selected Blank-holder pressure on the size of the buckles for reinforcement 1
- Figure 13: Sliding of tows for reinforcement 1
- Figure 14: Global analysis of the tetrahedron shape using reinforcement 2
- Figure 15: Global analysis of the tetrahedron shape using reinforcement 3



Figure 1: Architecture of reinforcement 1 at the scales of the fabric and the tow.

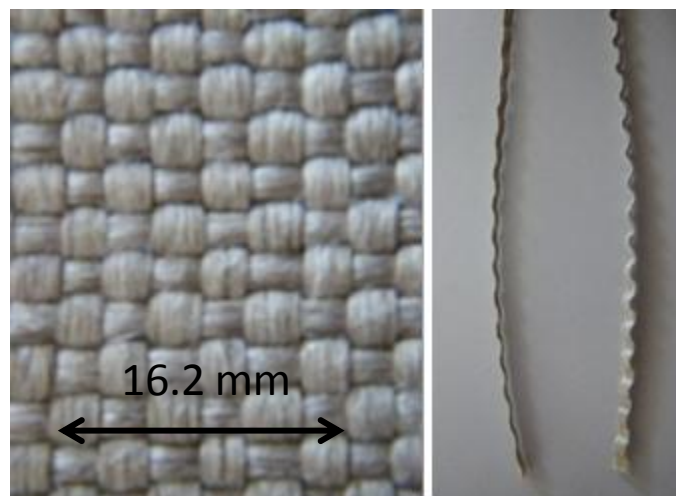


Figure 2: Architecture of reinforcement 2 at the scales of the fabric and the tow.

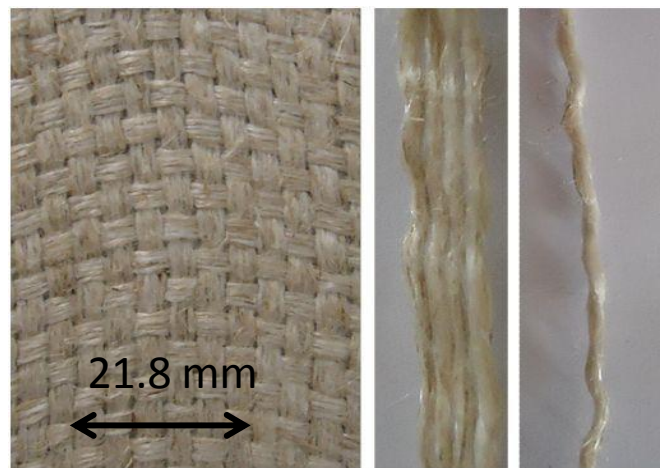


Figure 3: Architecture of reinforcement 3 at the scales of the fabric, the tow and the yarn.

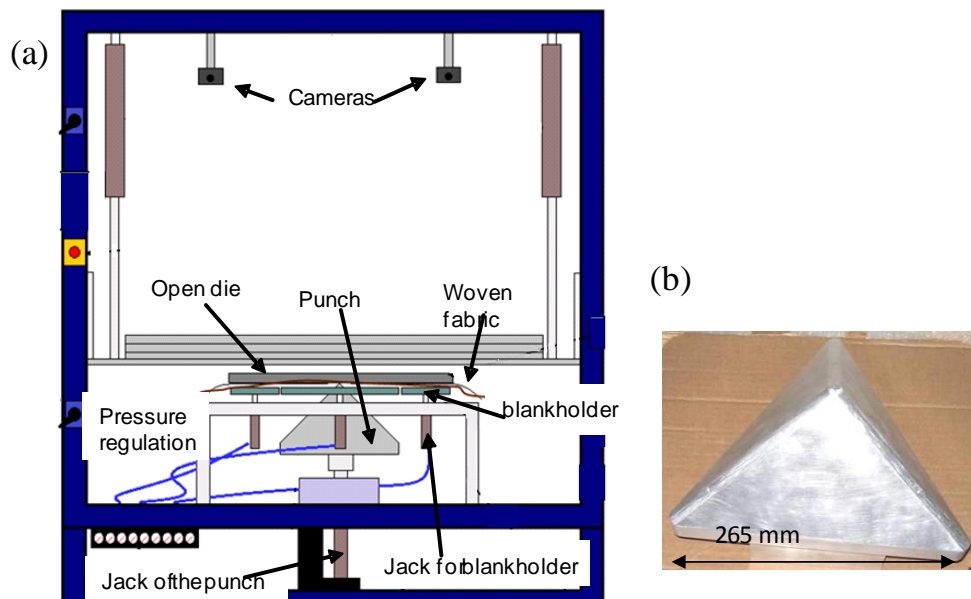
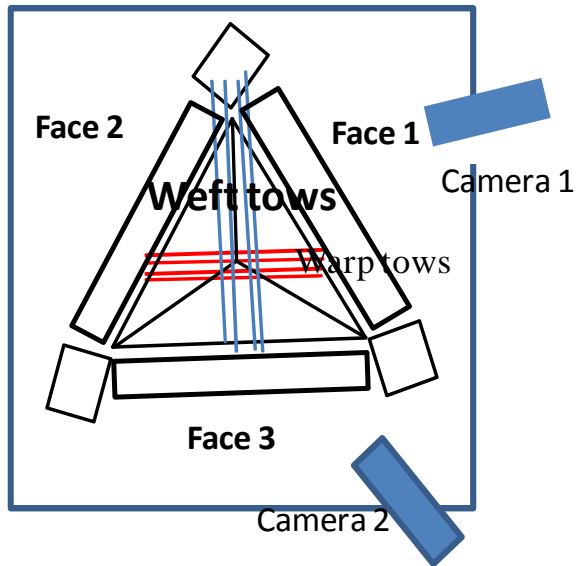
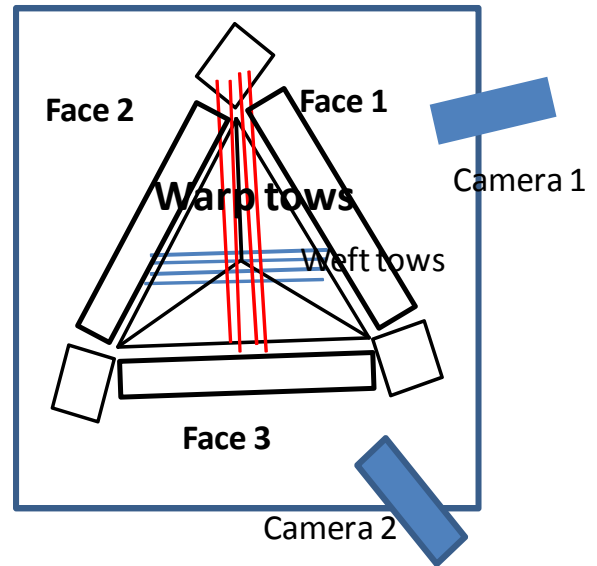


Figure 4: a) The sheet forming device and b) the tetrahedron punch

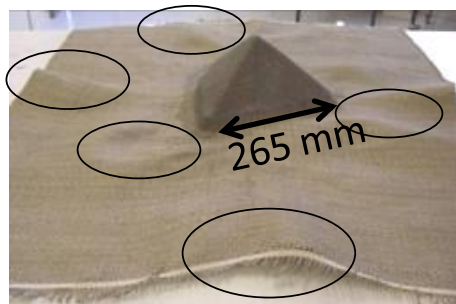


Orientation 0° Weft tows  
aligned with edge 1

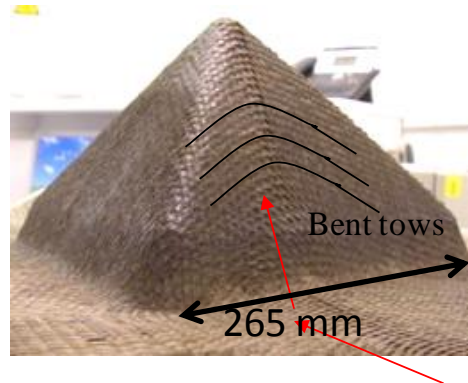


Orientation 90°: warp tows  
aligned with edge 1

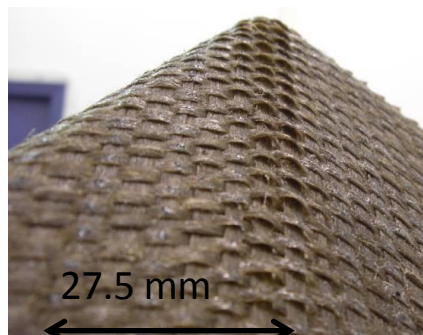
Figure 5: Initial positioning of the woven fabric



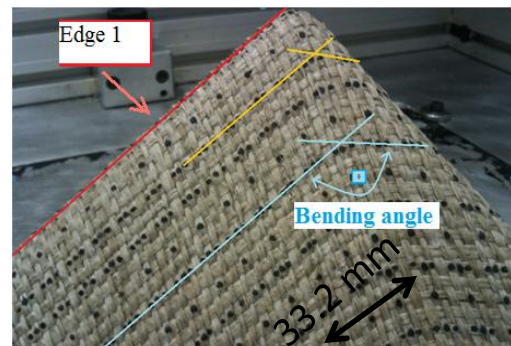
(a)



(b)



(c)



(d)

Figure 6: Forming of reinforcement 1: a) Wrinkles outside of the useful zone; (b) Position of the buckles and bending of the tows; (c) Focus on the buckles; (d) Measurement of the bending angle on Face 2



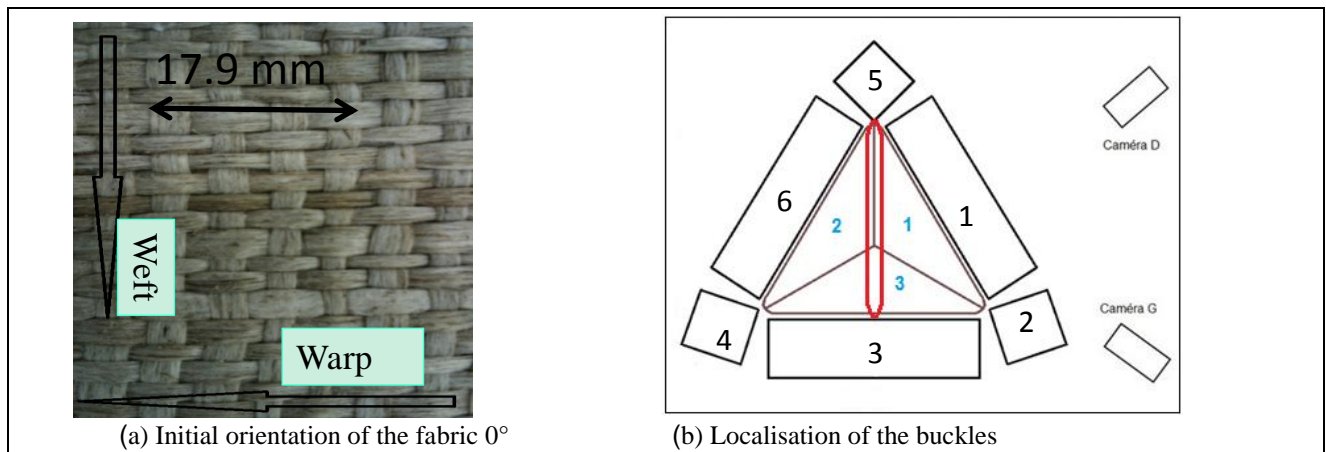


Figure 7: Localisation of the buckle zone for initial fabric orientation of  $0^\circ$

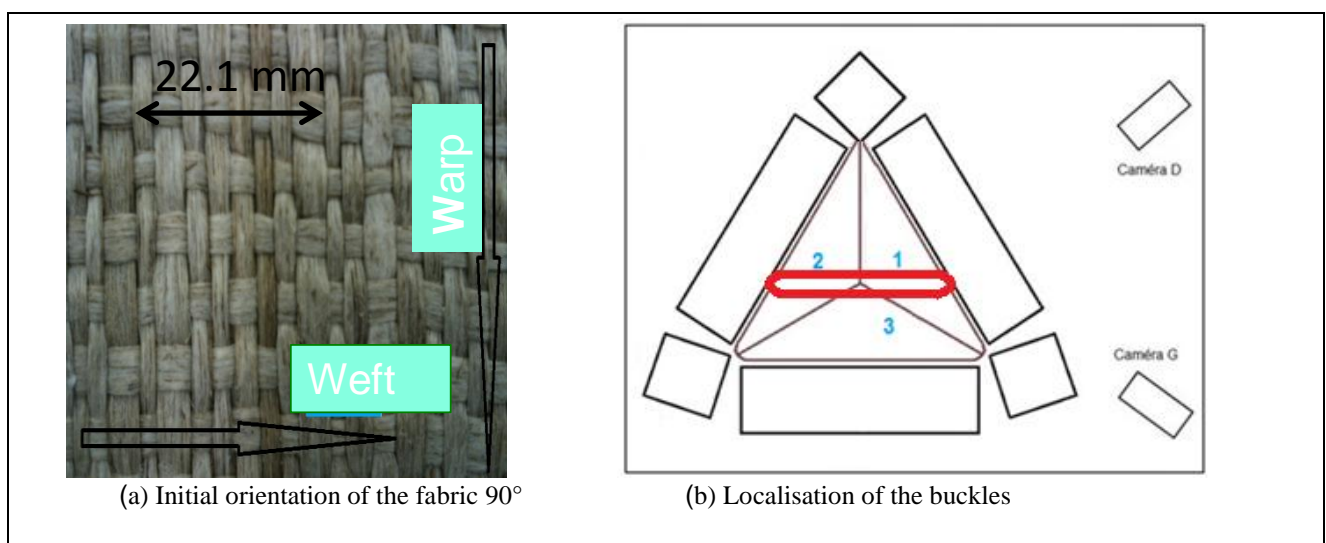


Figure 8: Localisation of the buckle zone for initial fabric orientation of  $90^\circ$

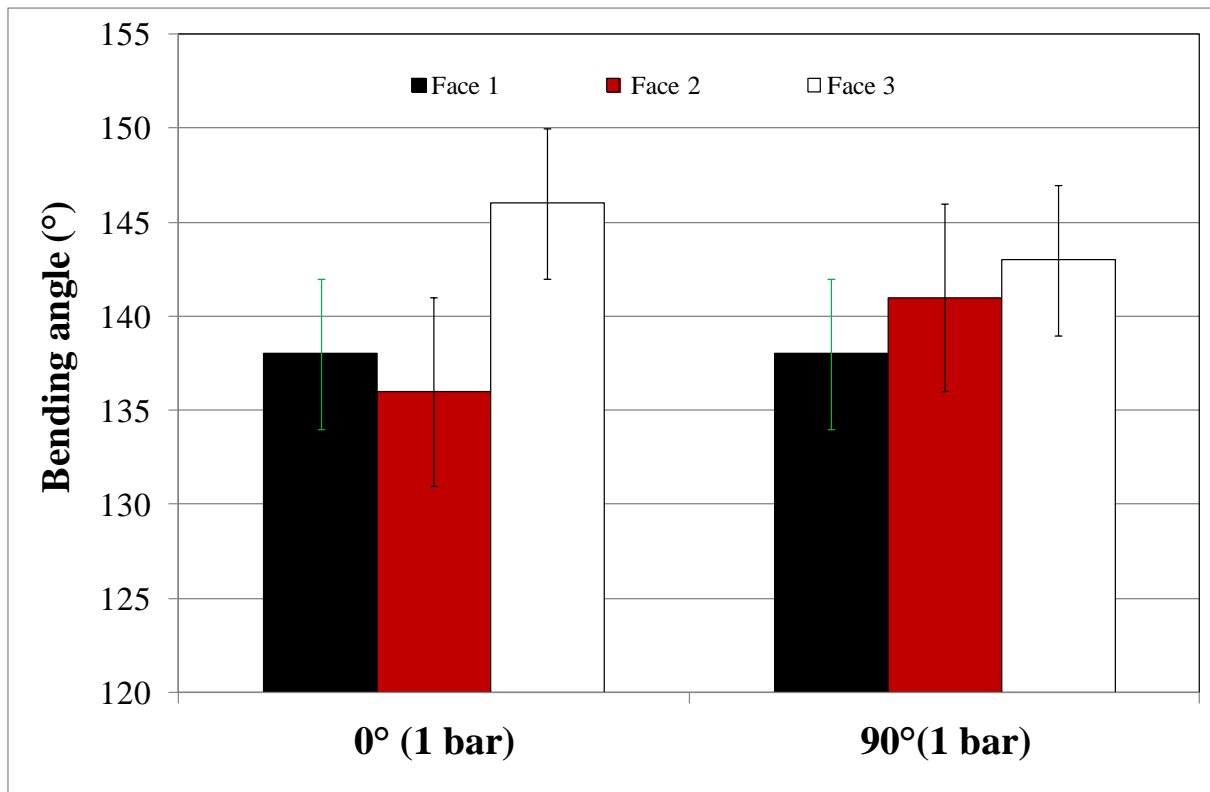


Figure 9: Influence of the initial fabric orientation on the tows curvature for reinforcement 1

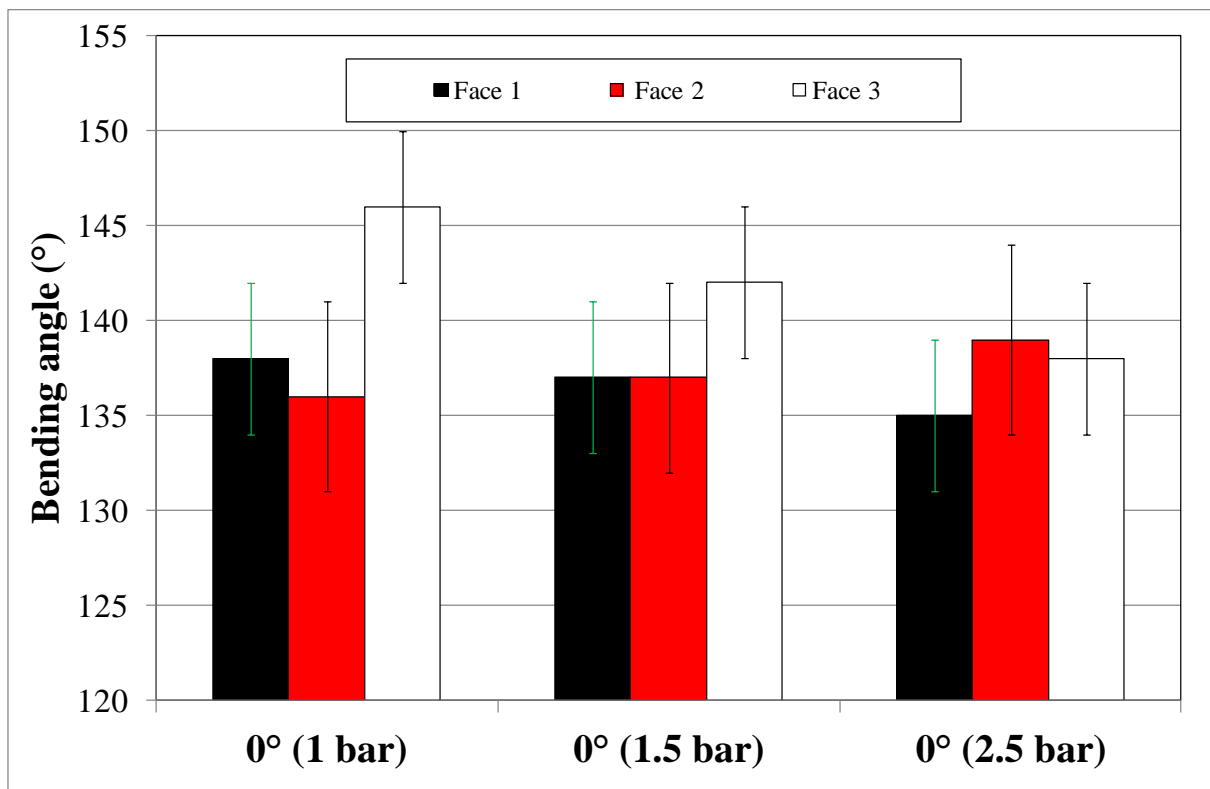


Figure 10: Influence of the global blank-holder pressure on the tows curvature for reinforcement 1

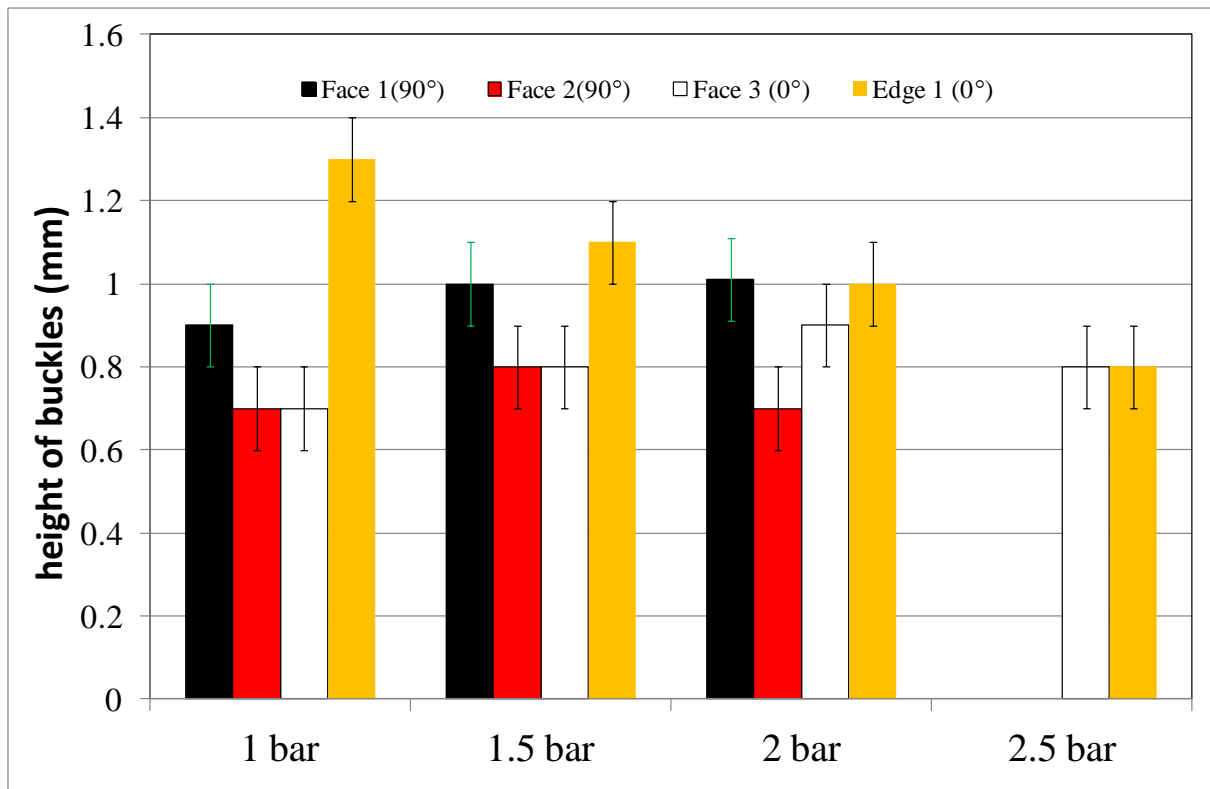


Figure 11: Influence of the initial fabric orientation and the global Blank-holder pressure on the size of the buckles for reinforcement 1

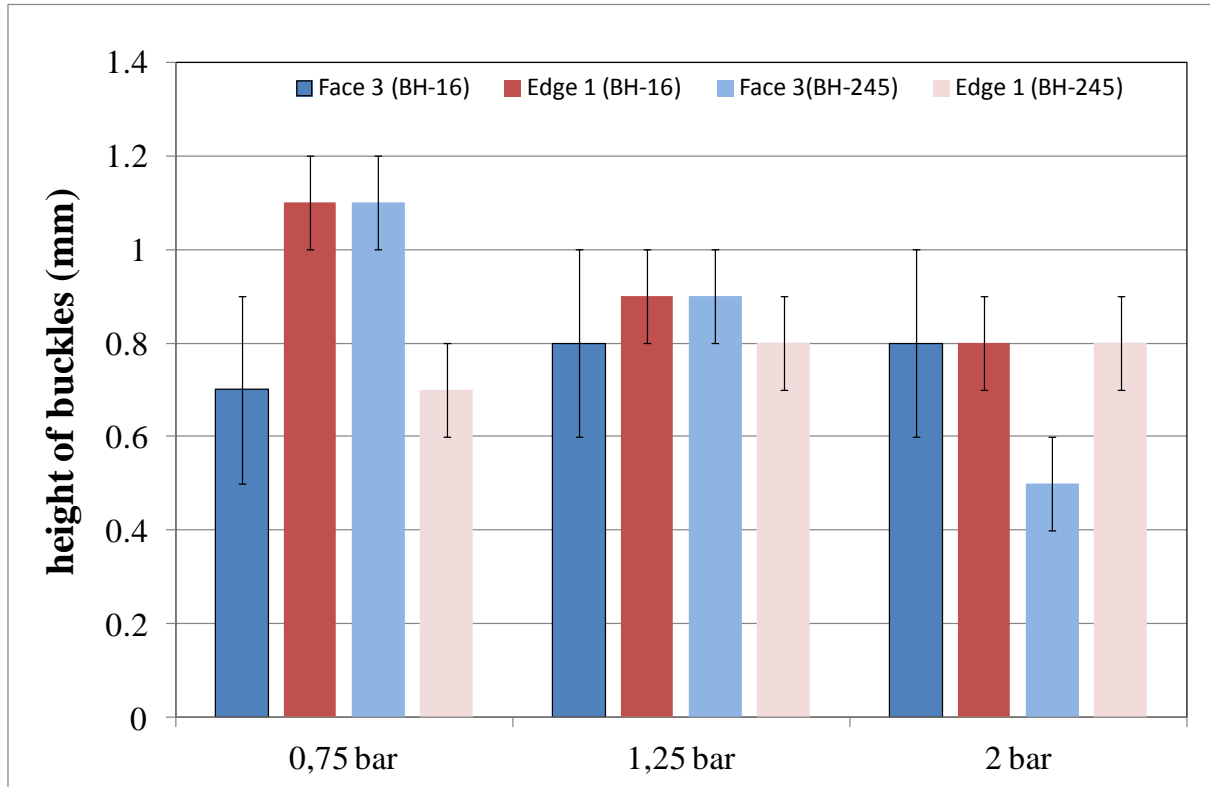


Figure 12: Influence of selected Blank-holder pressure on the size of the buckles for reinforcement 1

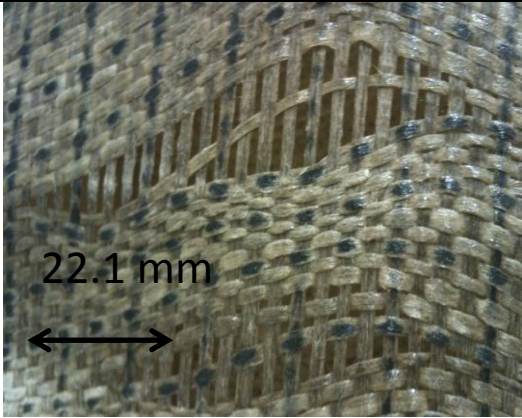
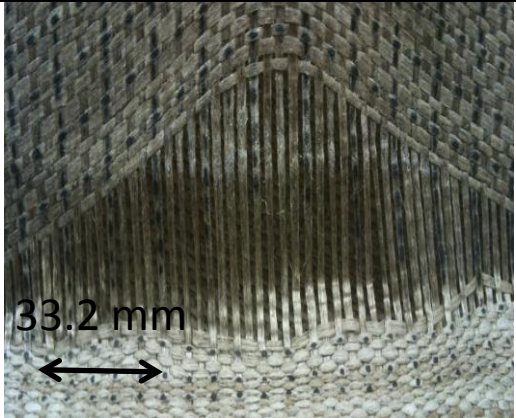
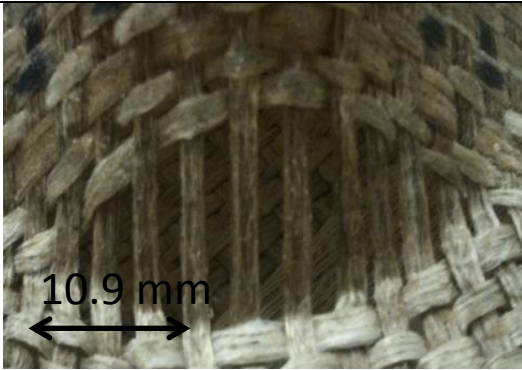
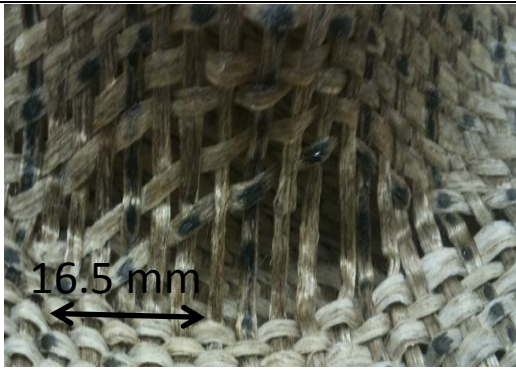
	2 bar blank-holder pressure	2.5 bar blank-holder pressure
Face 3 (under the buckles)	 <p>22.1 mm</p>	 <p>33.2 mm</p>
Bottom of the edge 1	 <p>10.9 mm</p>	 <p>16.5 mm</p>

Figure 13: Sliding of tows for reinforcement 1



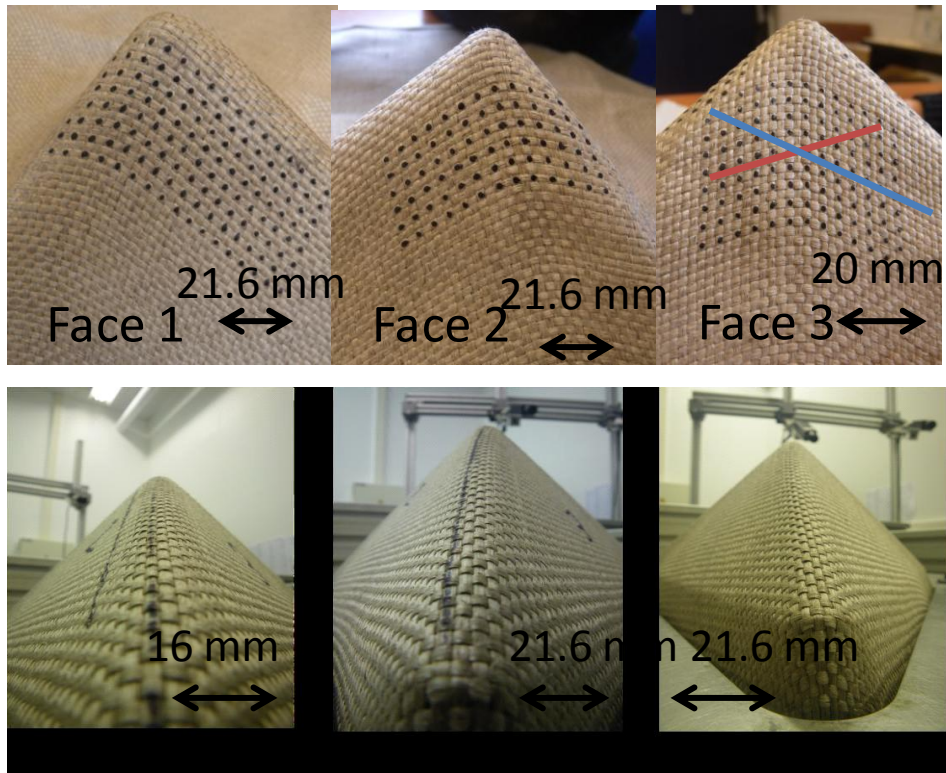


Figure 14: Global analysis of the tetrahedron shape using reinforcement 2

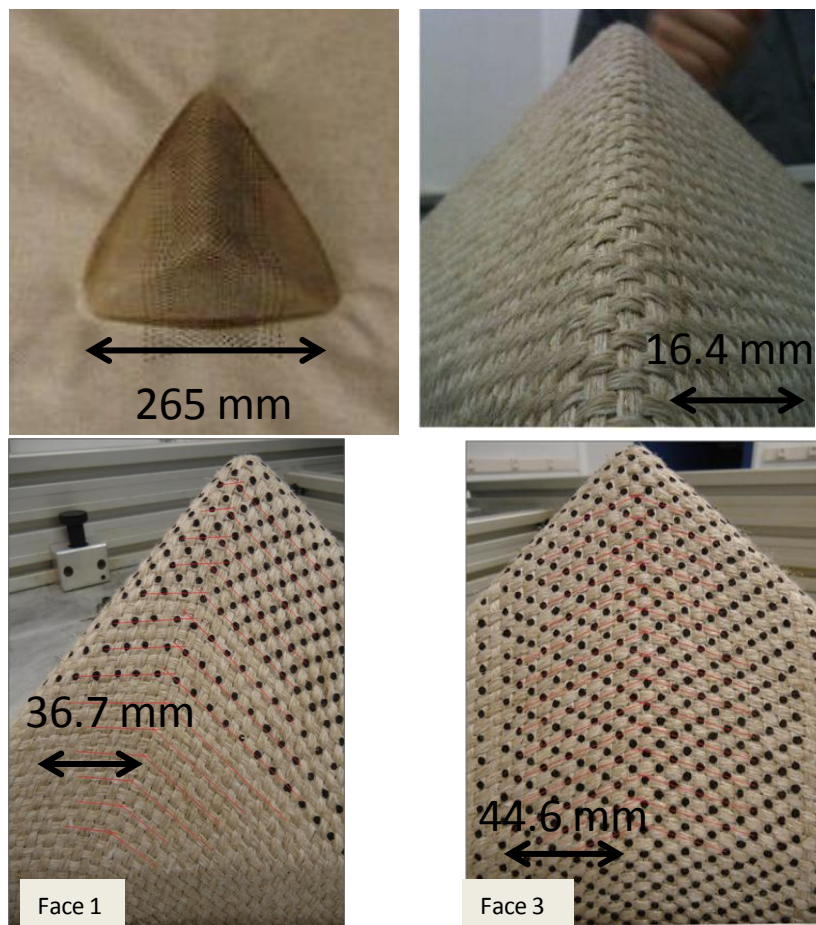


Figure 15: Global analysis of the tetrahedron shape using reinforcement 3